

## METHODS

# Simulation-Driven Triple-Tuned Array for $^1\text{H}$ , $^{31}\text{P}$ and $^{23}\text{Na}$ Using Composite Right- and Left-Handed Transmission Line for Rat Brain at 9.4T MRI

DANIEL HERNANDEZ<sup>1</sup>, MINYEONG SEO<sup>1</sup>, YEJI HAN<sup>2</sup>, AND KYOUNG-NAM KIM<sup>2</sup>

<sup>1</sup>Neuroscience Research Institute, Gachon University, Incheon 21988, Republic of Korea

<sup>2</sup>Department of Biomedical Engineering, Gachon University, Yeonsu-gu, Incheon 21936, South Korea

Corresponding author: Kyoungh-Nam Kim (kyoungnam.kim@gachon.ac.kr)


This work was supported in part by the KBRI Basic Research Program through Korea Brain Research Institute funded by the Ministry of Science and ICT under Grant 22-BR-05-02, and in part by the Institute for Information & Communications Technology Promotion (IITP) funded by the Korean Government (MSIP) for the Development of Precision Analysis and Imaging Technology for Biological Radio Waves under Grant 2021-0-00490.

**ABSTRACT** The use of ultrahigh-field-strength magnetic resonance imaging (MRI), such as 9.4T, is able to acquire multi-nuclear imaging with better image quality than lower field strengths. In particular the acquisition of sodium ( $^{23}\text{Na}$ ) or phosphorus ( $^{31}\text{P}$ ) images could benefit with higher signal-to-noise ratio (SNR). The design of radiofrequency RF coils is required to achieve a uniform field and to operate at the corresponding frequency. The general method to make multiple frequency coils has the drawback of using multilayers or reducing the size of the coils, which impose restriction on the utilization of space. For the conventional multiple frequency array, the design for the coil size imposes a challenge for the optimization of SNR and field intensity. In addition, the use of multiple coils increases the coupling between each coil. To circumvent these problems, we propose the use of composite right-left handed (CRLH) transmission lines (TL), which are able to resonate to multiple frequencies. This work demonstrates a design of an array of four channels, in which each channel consists of a single CRLH element capable to resonate at three frequencies corresponding to  $^1\text{H}$  at 400 MHz,  $^{31}\text{P}$  at 162 MHz, and  $^{23}\text{Na}$  at 105 MHz. The design was demonstrated with electromagnetic (EM) simulations and applied for rat brain for use in a 9.4T MRI system.

**INDEX TERMS** Composite right-handed and left-handed (CRLH), magnetic resonance imaging (MRI), small animal imaging, transmission line (TL).

## I. INTRODUCTION

Given the recent advances in technology, it is possible to perform magnetic resonance imaging (MRI) scans in small animals such as rats. Although scanning the brain of small animals remains challenging, there is great interest in conducting such studies to understand, for example, brain development during different life stages [1], [2] and using functional MRI (fMRI) to gain insights into cognitive and socio-emotional behaviors [2], [3], [4].

The associate editor coordinating the review of this manuscript and approving it for publication was Yi Zhang .

The primary source of signals in MRI is based on  $^1\text{H}$  nuclei, because it is the most common nucleus inside the human and animal bodies; however, there are other nuclei that can also be used to obtain MR images, such as sodium  $^{23}\text{Na}$  and phosphorus  $^{31}\text{P}$  [5]. Sodium and phosphorus nuclei are used to identify and measure physiological processes. Some of the applications of  $^{23}\text{Na}$  in MRI is to study tumors, strokes, multiple sclerosis, and neurodegenerative diseases [6], [7]. The predominant focus of  $^{31}\text{P}$  MRI is to provide information on the bioenergetics of the human brain, that is, to show the changes in the concentrations and ratios of phosphocreatine (PCr), adenosine triphosphate (ATP), and intracellular pH.

This information is useful for analyzing neurological diseases such as Parkinson's and Alzheimer's [8].

The challenges in using sodium and phosphorus in MRI include the low signal-to-noise ratio (SNR) as well as the low spatial and temporal resolution owing to their low concentrations within the human body in comparison to <sup>1</sup>H concentrations, which are abundant in the human body. Additionally, sodium and phosphorus have a lower resonance frequency; in comparison, <sup>1</sup>H has a gyromagnetic ratio  $\gamma$  (MHz/T) of 42.58, whereas the corresponding values for <sup>31</sup>P and <sup>23</sup>Na are 17.25 and 11.27, respectively [5]. Consequently, the operational frequencies of the RF coils designed to operate with a 9.4T MRI system are 400, 162, and 105 MHz for <sup>1</sup>H, <sup>31</sup>P, and <sup>23</sup>Na, respectively.

There is ongoing research on the optimal coil configuration and geometry that would produce a high-intensity  $|B_1^+|$  field with a uniform magnetic flux density for small animal and multi-nuclei imaging [9], [10]. Double and triple resonance coils have also been proposed [11], [12], [13], which are preferred because they offer a high SNR for the <sup>31</sup>P, and <sup>23</sup>Na frequencies without any adverse effect on the high performance of <sup>1</sup>H imaging. Although, simultaneous multi-nuclei imaging is limited due to the MRI RF amplifiers and gradient coils, it is beneficial to have a coil that can acquired images of multi-nuclei, since it helps the registration of images, localization of tissues or organs and reduce the time for setting up the scanning procedure. The latter is true when considering animal imaging, which most of the time require anesthesia and other measurement devices.

A major challenge in implementing multiple frequency RF coils is space. One typical setup is to use loop-array coils arranged in a cylindrical shape, in which the size of the individual loop coils should be reduced so that all coils could fit. However, this setup has several disadvantages. Mutual coupling between the array coils must be minimized, and the field intensity is affected by the size of the coil and the distance between the RF coil and the imaging body [14]. To solve this issue, we propose the use of composite right- and left-hand (CRLH) transmission lines (TLs). The CRLH TLs have been shown to enhance the image characteristics in comparison to the traditional TLs. In addition, they can be used to produce uniform  $|B_1^+|$  fields and low coupling between the TL elements [15], [16] and can produce multiple resonance frequencies [17].

In this study, we propose the use of an array of CRLH TLs in a volumetric arrangement in combination with a four-channel array coil to produce a  $|B_1^+|$  field across the rat's brain for <sup>1</sup>H, <sup>31</sup>P, and <sup>23</sup>Na in a 9.4T MRI system. Compared to the microstrip TLs, the CRLH TLs have the ability to produce a multiple frequency uniform field along the main magnetic field axis (z-axis) and axial plane (x-y plane) independent of the physical length. Primarily, the independence of the physical length of the TL from the operating signal wavelength makes the CRLH TL a good option for developing Tx coils for small animals and multiple frequency

coils. The proposed design has the advantage that can produce uniform field for the three selected frequencies, while using the same space, in addition to low coupling between elements. The size of the CRLH TL is reduced to accommodate the rat brain size.

## II. MATERIALS AND METHODS

### A. CRLH THEORY

The use of traditional TL and microstrips have been proposed for MRI. However, because the maximum wave field produced occurs when the length of the TL is half the wavelength, their performance is directly related to their electric length, which is a limitation. Recent research on the use of CRLH TL suggests that these RF elements can be modified to perform at any length, and MRI applications have also been reported [18], [19], [20].

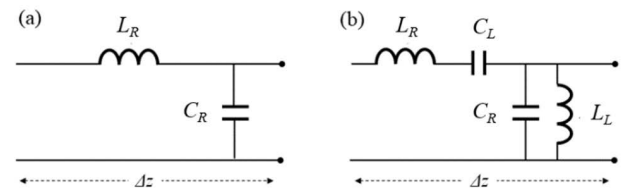


FIGURE 1. (a) Circuit diagram of the conventional transmission line and (b) the CRLH transmission line.

As shown in Fig. 1(a), the traditional TL is represented by a series inductance  $L_R$  that is connected in parallel to capacitance  $C_R$  varying in space  $\Delta z$ ; suffix  $R$  represents the right-hand properties. The electrical length of a traditional TL is given by the following equation for propagation constant:

$$\gamma = \sqrt{(j\omega L_R)(j\omega C_R)} \quad (1)$$

In addition, the characteristic impedance is expressed as

$$Z_0 = \sqrt{(j\omega L_R)/(j\omega C_R)} \quad (2)$$

From the above equations, it can be seen that the propagation constant and characteristic impedance depend only on the geometry of the transmission line. Consequently, the electrical length at certain frequencies works out to be an impractical distance. As mentioned previously, the advantage of the CRLH TL is that the electrical length can be modified to fulfill the desired geometry. As shown in Fig. 1(b), certain modifications such as the addition of series capacitance  $C_L$  and parallel inductance  $L_L$  to the traditional TL are required. The resulting propagation constant is given by

$$\gamma = \alpha + j\beta = \sqrt{Z'Y'} \quad (3)$$

$$Z'(\omega) = j\left(\omega L'_R - (\omega C'_L)^{-1}\right) \quad (4)$$

$$Y'(\omega) = j\left(\omega C'_R - (\omega L'_L)^{-1}\right) \quad (5)$$

In addition, the characteristic impedance is expressed as

$$Z_0^{unbal} = Z_L \sqrt{(L'_R C'_L \omega^2 - 1)/(L'_L C'_R \omega^2 - 1)} \quad (6)$$

Here,  $Z_0^{unbal}$  is  $Z_0^{unbalanced}$ . These equations demonstrate that the propagation constant and characteristic impedance can be modified by changing the inductance and capacitance values, and hence, they are dependent on the frequency. Consequently, a reduction in size of the CRLH TL is possible, thereby making it useful for small-animal MRI applications; this is especially true for transmission elements, given the advantages that the transmission lines have to be decoupled in correspondence with the loop coil elements [21], [22]. By solving the equations to find the possible frequencies  $\omega$ , it is clear that at least two frequencies are present [23].

$$\omega_1 = (\sqrt{L_R C_L})^{-1} \quad (7)$$

$$\omega_2 = (\sqrt{L_L C_R})^{-1} \quad (8)$$

**B. MULTI-TUNED CRLH DESIGN**

Each CRLH element is composed of two layers of copper lines; the top layer that carries the electric current is 15 mm wide and 40 mm long, while the ground line is 30 mm wide for the same length. The top line has two gaps of 2 mm to include a series capacitor and inductor. Both copper lines were placed between a dielectric material of 5 mm thickness, 30 mm width, and 40 mm length. Fig. 2a shows the geometry of this configuration. Series capacitors and inductors were added between the gaps, and parallel capacitors and inductors were added at both sides of the transmission line, on both the left and right sides. The array consisted of four elements arranged in a cylindrical shape covering the rat brain, as illustrated in Fig. 2b. The cylinder had a radius of 40 mm, and each element was rotated 90° from the other. Figure 2b shows the label for each channel number and indicates that the CRLH operates for <sup>1</sup>H, <sup>31</sup>P and <sup>23</sup>Na or equivalent to operational frequency of 400, 162 and 105 MHz

**C. REFERENCE COIL MODEL**

To evaluate the performance of the proposed CRLH design, we have also added a reference loop coil array for each frequency. The total array consists of twelve loop coils of 20 mm wide and 40mm of length each, this size was chosen to fit around a circumference of 100 mm diameter. Four coils were assigned to operate at 400 MHz for <sup>1</sup>H, four channels for <sup>31</sup>P at 162 MHz and four coils operating for <sup>23</sup>Na at 105 MHz. Figure 2c shows the reference coil array for triple tuned frequency with the rat head model, and the labels for each channel and operation frequency. Each coil was separated by 30° from each other to reduce the coupling between coils and to fit the space. Each coil has a single tuning capacitor.

**D. RAT MODEL**

The rat model used in the simulations was part of the ViZOO library provided by the simulation software *Sim4Life* (MedTech AG, Zurich) [24]. The rat model is based on a male Sprague Dawley® rat weighing 567 g, 260 mm long excluding its tail, and containing 51 tissues. The electrical properties (EP) of each tissue were assigned based

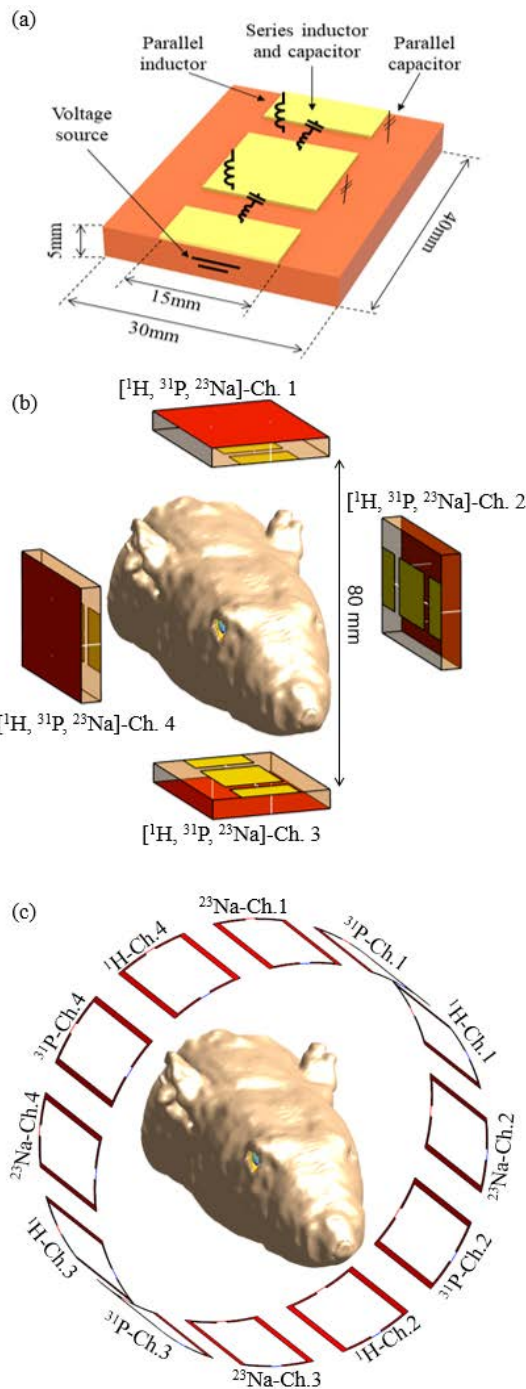


**FIGURE 2. (a) Model of a single CRLH TL with corresponding dimensions and the position of the capacitors and inductors; (b) Model of the CRLH array indicating each of the channels and the position of rat head, (c) the reference loop array coil consisting of twelve loop coils, each coil is labeled for the corresponding nuclei and channel number.**

on the dataset provided by the software for each operation frequency. In the case of the cerebellum, EP at 400 MHz frequency is given as 1.03 S/m conductivity and 55.99 permittivity. The corresponding conductivity and permittivity values at 162 and 105 MHz are 0.867 S/m and 72.34 and 0.79 S/m and 87.57, respectively.

**E. SIMULATIONS SET-UP**

Magnetic  $|B_1^+|$  field distributions were obtained for the rat brain with the proposed models using commercial electromagnetic (EM) simulation software (Sim4life, Zurich, MedTech AG (ZMT)). To tune a single CRLH, a Gaussian pulse with a central frequency ( $f_c$ ) of 400 MHz and bandwidth of 800 MHz was used as the source to enable visibility of the lower frequencies as well. For the case of the array simulation loaded with the rat, individual simulations were performed with  $f_c$  corresponding to 400, 162, and 105 MHz with bandwidth at twice that of  $f_c$ . All conductor materials were set as perfect electric conductors (PEC). The EP of the dielectric material used for the CRLH TLs were 0.0038 S/m and 4 for conductivity and relative permittivity, respectively, corresponding to FR-4. The overall impedance of each TL was matched to  $50 \Omega$  by adding an inductor and capacitor network to the excitation terminals located at one end of the TL. The reference loop array was also tuned to the correspondent frequencies and matched each channel to  $50 \Omega$ .

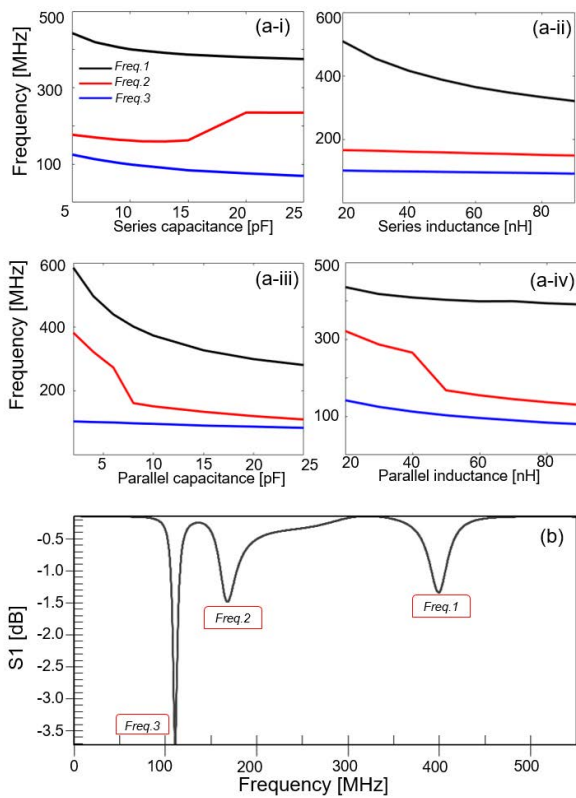


**FIGURE 3.** Variation in high (Freq. 1), middle (Freq. 2) and low (Freq. 3) frequencies with respect to (a-i) series capacitor, (a-ii) series inductance, (a-iii) parallel capacitance, and (a-iv) parallel inductance. (b) Triple resonance frequency from a single CRLH element before matching.

**III. RESULTS**

A multi-tuned CRLH array configuration consisting of four elements for the multi-nuclei ( $^1\text{H}$ ,  $^{31}\text{P}$ , and  $^{23}\text{Na}$ ) was designed, as described in the previous section. Tuning of a

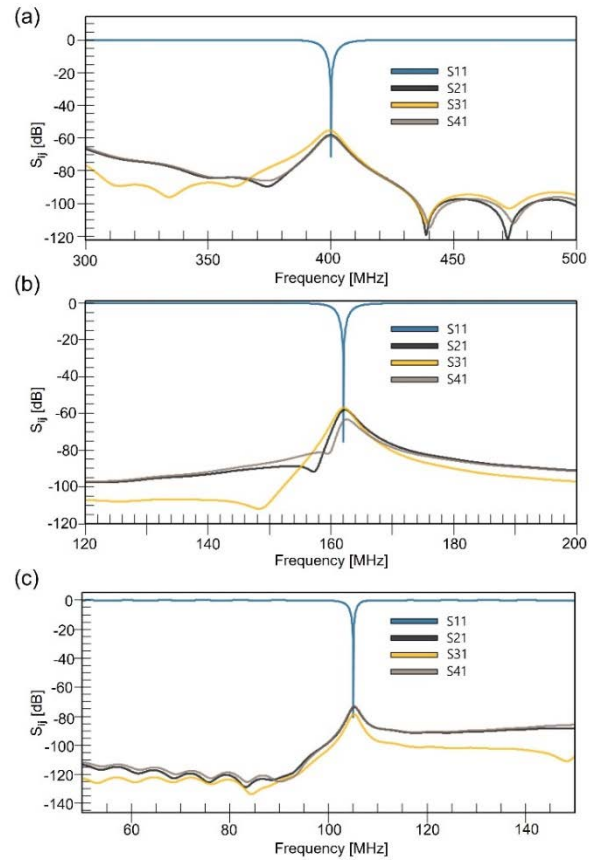


**FIGURE 4.** The coupling analysis with the  $S_{ij}$  parameters between elements of the CRLH array showing low coupling at (a) 400 MHz, (b) 162 MHz (c) and 105 MHz.

single TL element was performed to determine the values of the capacitors and inductors to achieve the desired resonance frequencies. The proposed design consists of four types of lumped elements: a series capacitor and inductor along with a set of parallel capacitor and inductors. Figure 3a illustrates the effect of variation in the value of each component on the resonance frequency. It can be observed that the change in the value of the parallel capacitor (Figure 3a-iii) has a strong impact on the highest frequency, that is, Freq. 1 in the plots, whereas the same capacitor has no influence on the lowest frequency (Freq. 3). Furthermore, the parallel inductance and series capacitor can be used to tune Freq. 3, while Freq. 2 remains constant and unaffected by any change in value of the series inductance (Fig. 3a-ii).

The evaluation of the coupling between elements of the four-channel CRLH array, are plotted in Fig. 4, showing the  $S_{ij}$  parameters, the tuning and matching for each frequency of the CRLH array. Individual matching circuits were applied for each frequency simulation to obtain  $50 \Omega$  impedance. The CRLH elements exhibited low coupling between each other, with values between  $-60$  and  $-80$  dB.

Given the fact that the same TL was used for multiple frequencies, there is no interference between the elements

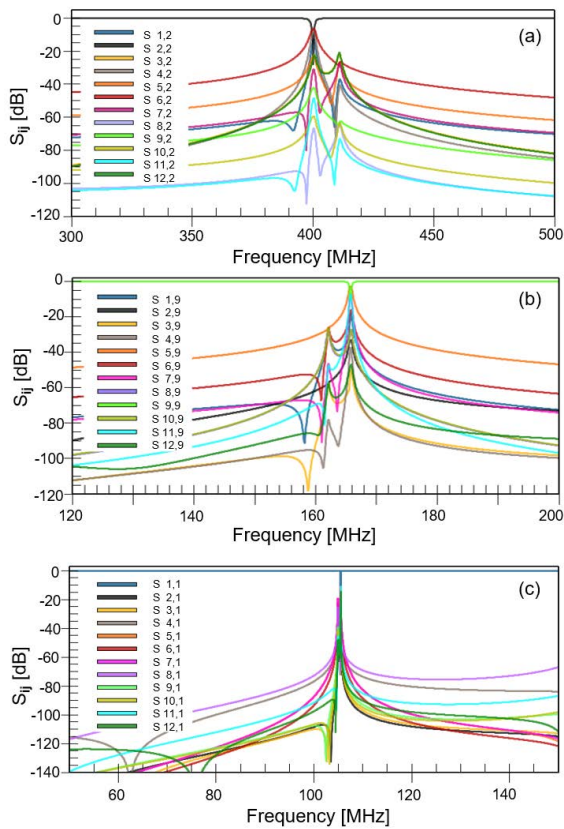


**FIGURE 5.** The  $S_{ij}$  parameters acquired with the reference loop array at (a) 400 MHz, (b) 162 MHz; (c) and 105 MHz, showing poor coupling between elements.

at their operating frequencies, as is the case when using separate loop coils. The frequency variations due to the parallel capacitance and inductance are plotted in Fig. 3a-iii and Fig. 3a-iv, respectively. The resonance of a single unloaded CRLH TL was achieved with a series capacitor of 8 pF and series inductor of 45 nH in combination with parallel capacitors and inductors of 9 pF and 50 nH, respectively. The  $S_{11}$  parameters showing the three resonance frequencies are shown in Figure 3b.

For the case of the reference loop array coil, the coupling between the elements is shown in Fig. 5 by plotting the  $S_{ij}$  parameters. For the reference loop array operating at 400 MHz (Fig. 5a) the  $S_{ij}$  parameter had a minimum of  $-5$  dB, while the CRLH array (Fig. 4a) had  $-56$  dB. For the frequency of 162 MHz the reference array (Fig. 5b) and the proposed CRLH array (Fig. 4b) had  $S_{ij}$  parameters of  $-3$  dB and  $-61$  dB, respectively. Lastly, the frequency of 105 MHz had minimum  $S_{ij}$  of  $-10$  dB and  $-68$  dB for the reference and CRLH array, respectively. These results indicate that the proposed design have low coupling between elements. Although, adding a decoupling method to the reference loop array can improve the  $S_{ij}$  parameters, the proposed CRLH array do not require additional decoupling methods.

The magnetic  $|B_1^+|$  fields obtained using the rat model in the axial planes are shown in Fig. 6. The field maps

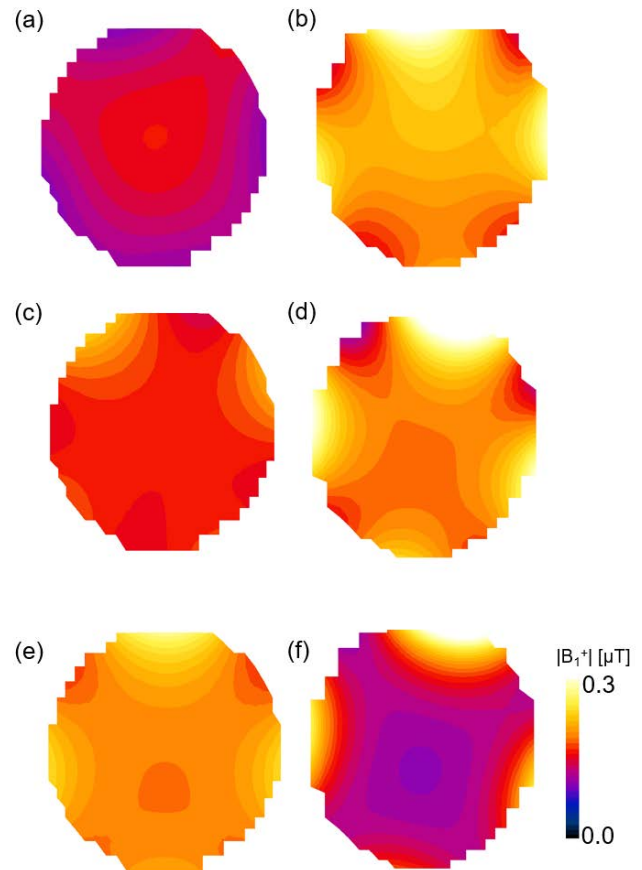


**FIGURE 6.** The  $|B_1^+|$  field of the rat head in the X-Y plane, acquired at 400 MHz intended for  $^1\text{H}$  (a) loop array, (b) CRLH array. The  $|B_1^+|$  field at 162 MHz for  $^{31}\text{P}$  with (c) loop array, (d) CRLH array. And the  $|B_1^+|$  field at 105 MHz for  $^{23}\text{Na}$  with (e) loop array, (f) CRLH array.

corresponding to  $^1\text{H}$  or 400 MHz the field maps are displayed in Fig. 6a-b for the reference loop coil and the proposed CRLH array, respectively, where it can be seen that the field intensity with the proposed array has higher field intensity than the reference. The mean value of the field at 400 MHz was  $0.12$  and  $0.21$   $\mu\text{T}$ , respectively, the low field from the loop array corresponds to the reduced size of the loop coil. The maps for  $^{31}\text{P}$  at 162 MHz are displayed in Fig. 6c-d for the loop and CRLH array, respectively, in which it can be noticed that the field produced by the CRLH has also higher intensity, which had a mean value of  $0.20$   $\mu\text{T}$ , while the loop array had a mean of  $0.15$   $\mu\text{T}$ . Lastly, the field maps for  $^{23}\text{Na}$  at 105 MHz are displayed in Fig. 6e-f, for the reference and the CRLH array, respectively, in this case the intensity of the CRLH array is lower than the reference, the CRLH array had a mean value of  $0.14$   $\mu\text{T}$ , whereas, the loop array had a mean value of  $0.19$   $\mu\text{T}$ .

In particular, as the region of interest is the brain of the rat, Fig. 7a-c highlights the  $|B_1^+|$  field of the cerebellum, cerebral hemisphere, CSF, and midbrain of the rat, for 400, 162 and 105 MHz, respectively, computed with the CRLH array. Figure 7d summarizes the  $|B_1^+|$  field mean value for

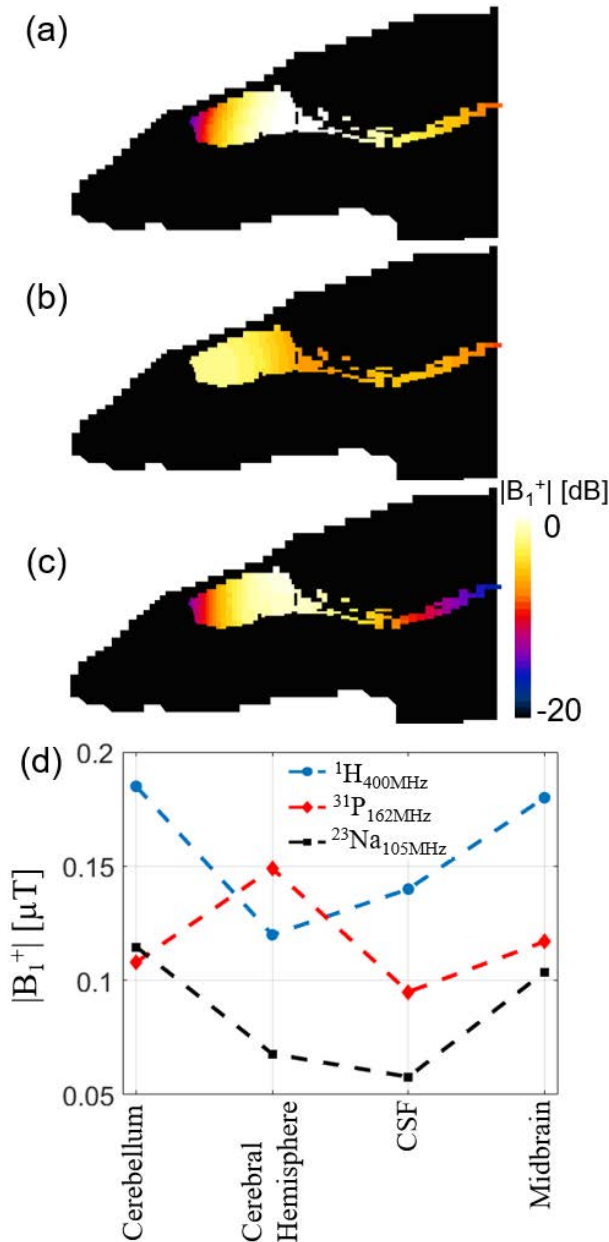


**FIGURE 7.** The  $|B_1^+|$  field in Z-Y plane acquired with the CRLH array highlighting the main rat brain tissues (cerebellum, cerebral hemisphere, CSF and midbrain) for (a) 400 MHz intended for  $^1\text{H}$ , (b) 162 MHz for  $^{31}\text{P}$  and (c) 105 MHz for  $^{23}\text{Na}$ . The volumetric  $|B_1^+|$  field mean value in each tissue and frequency.

each frequency and the selected tissues (cerebellum, cerebral hemisphere, CSF, and midbrain). The simulations indicate that CRLH based coil array is capable of producing  $|B_1^+|$  field at the three selected frequencies and could be used for 9.4T MR imaging of multi-nuclei rat brain.

**IV. DISCUSSION AND CONCLUSION**

We designed and performed EM simulations of a novel triple-tuned RF coil using a CRLH TL array for  $^1\text{H}$ ,  $^{31}\text{P}$ , and  $^{23}\text{Na}$ . This is a preceding work using metamaterials as array coils

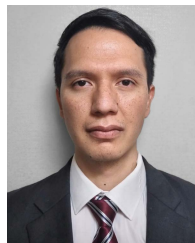
that established their capability to generate strong fields at multiple resonance frequencies for use in small animals such as rats. The results from the simulations show that CRLH arrays are capable of producing strong fields comparable to a reference loop coil array and demonstrate that a triple tuning frequency is possible. The proposed CRLH array provide the advantage to use the same resonator for three frequencies, allowing to use the space more efficiently, contrary to the conventional multi frequency loop coil array, where the size of the loop coils should be considered to accommodate to the available space. The coupling between the elements of the CRLH array had low interaction, in contrast to the reference loop array, where dedicated decoupling method should be used. The difference in field intensity at each frequency can be attributed to the frequency dependence of the electrical properties of the tissues and wavelength propagation. One of the limitations of the proposed design is the use of additional lumped elements, compared to a loop coil. In practice the selection of the capacitor and inductor values for the desired frequencies could be an exhausting process, but variable capacitors and inductors could simplify the tuning process. We hope that this novel work can be utilized in the future to design and develop improved array coils for MRI applications requiring high-frequency and multi-nuclei imaging in small animals.

Based on the proposed design, the next step would be to develop the proposed elements and to design a similar array concept for human brain imaging combining  $^1\text{H}$  and multi-nuclei. The design for human application, would require to optimize the size of the CRLH TL to resonate at the desired frequencies, in addition, it would be possible to add more channels, for better field intensity and uniformity. Modifications to the geometry and tuning capacitors could be made for achieving resonance frequencies for other nuclei of interest, such as  $^{19}\text{F}$ ,  $^3\text{He}$ , or  $^{129}\text{Xe}$ .

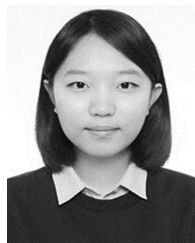
**REFERENCES**

- [1] M. S. Stringer, H. Lee, M. T. Huuskonen, B. J. MacIntosh, R. Brown, A. Montagne, S. Atwi, J. Ramirez, M. A. Jansen, I. Marshall, S. E. Black, B. V. Zlokovic, H. Benveniste, and J. M. Wardlaw, "A review of translational magnetic resonance imaging in human and rodent experimental models of small vessel disease," *Transl. Stroke Res.*, vol. 12, no. 1, pp. 15–30, Feb. 2021, doi: 10.1007/s12975-020-00843-8.
- [2] I. Brusini, E. MacNicol, E. Kim, Ö. Smedby, C. Wang, E. Westman, M. Veronese, F. Turkheimer, and D. Cash, "MRI-derived brain age as a biomarker of ageing in rats: Validation using a healthy lifestyle intervention," *Neurobiol. Aging*, vol. 109, pp. 204–215, Jan. 2022, doi: 10.1016/j.neurobiolaging.2021.10.004.
- [3] S. Terbeck, J. Savulescu, L. P. Chesterman, and P. J. Cowen, "Noradrenaline effects on social behaviour, intergroup relations, and moral decisions," *Neurosci. Biobehav. Rev.*, vol. 66, pp. 54–60, Jul. 2016, doi: 10.1016/j.neubiorev.2016.03.031.
- [4] P. Stenroos, J. Paasonen, R. A. Salo, K. Jokivarsi, A. Shatillo, H. Tanila, and O. Gröhn, "Awake rat brain functional magnetic resonance imaging using standard radio frequency coils and a 3D printed restraint kit," *Frontiers Neurosci.*, vol. 12, p. 548, Aug. 2018, doi: 10.3389/fnins.2018.00548.
- [5] R. Hu, D. Kleimaier, M. Malzacher, M. A. Hoesl, N. K. Paschke, and L. R. Schad, "X-nuclei imaging: Current state, technical challenges, and future directions," *J. Magn. Reson. Imag.*, vol. 51, no. 2, pp. 355–376, 2020, doi: 10.1002/jmri.26780.

- [6] G. C. LaVerde, C. A. Jungreis, and E. Nemoto, "Sodium time course using  $^{23}\text{Na}$  MRI in reversible focal brain ischemia in the monkey," *J. Magn. Reson. Imag.*, vol. 30, no. 1, pp. 219–223, 2009, doi: [10.1002/jmri.21723](https://doi.org/10.1002/jmri.21723).
- [7] G. Madelin and R. R. Regatte, "Biomedical applications of sodium MRI *in vivo*," *J. Magn. Reson. Imag.*, vol. 38, no. 3, pp. 511–529, Sep. 2013, doi: [10.1002/jmri.24168](https://doi.org/10.1002/jmri.24168).
- [8] J. Ren, " $^{31}\text{P}$ -MRS of healthy human brain: ATP synthesis, metabolite concentrations, pH, and  $T_1$  relaxation times," *NMR Biomed.*, vol. 28, no. 11, pp. 1455–1462, 2015, doi: [10.1002/nbm.3384](https://doi.org/10.1002/nbm.3384).
- [9] B. Gruber, M. Froeling, T. Leiner, and D. W. J. Klomp, "RF coils: A practical guide for nonphysicists," *J. Magn. Reson. Imag.*, vol. 48, no. 3, pp. 590–604, Sep. 2018, doi: [10.1002/jmri.26187](https://doi.org/10.1002/jmri.26187).
- [10] C. Wang, Y. Li, B. Wu, D. Xu, S. J. Nelson, D. B. Vigneron, and X. Zhang, "A practical multinuclear transceiver volume coil for *in vivo* MRI/MRS at 7 T," *Magn. Reson. Imag.*, vol. 30, no. 1, pp. 78–84, 2012, doi: [10.1016/j.mri.2011.08.007](https://doi.org/10.1016/j.mri.2011.08.007).
- [11] E. J. Kim, D. Kim, S. Lee, and D. Heo, "Development of  $^1\text{H}$ - $^{31}\text{P}$  animal RF coil for pH measurement using a clinical MR scanner," *J. Korean Soc. Magn. Reson. Med.*, vol. 18, no. 1, pp. 52–58, 2014, doi: [10.13104/jksmrm.2014.18.1.52](https://doi.org/10.13104/jksmrm.2014.18.1.52).
- [12] S.-D. Han, J. Song, D. Hernandez, and K.-N. Kim, "Dual-tuned monopole/loop coil array for concurrent RF excitation and reception capability for MRI," *J. Korean Phys. Soc.*, vol. 75, no. 8, pp. 610–616, Oct. 2019, doi: [10.3938/jkps.75.610](https://doi.org/10.3938/jkps.75.610).
- [13] S.-D. Han, P. Heo, H.-J. Kim, H. Song, D. Kim, J.-H. Seo, Y. Ryu, Y. Noh, and K.-N. Kim, "Double-layered dual-tuned RF coil using frequency-selectable PIN-diode control at 7-T MRI," *Concepts Magn. Reson. B, Magn. Reson. Eng.*, vol. 47B, no. 4, Oct. 2017, Art. no. e21363, doi: [10.1002/cmr.b.21363](https://doi.org/10.1002/cmr.b.21363).
- [14] D. Hernandez and K. N. Kim, "A review on the RF coil designs and trends for ultra high field magnetic resonance imaging," *Investig. Magn. Reson. Imag.*, vol. 24, no. 3, pp. 95–122, May 2020, doi: [10.13104/imri.2020.24.3.95](https://doi.org/10.13104/imri.2020.24.3.95).
- [15] A. Lai, C. Caloz, and T. Itoh, "Microwave devices based on composite right/left-handed (CRLH) transmission line metamaterials," in *Proc. IEEE Int. Workshop Antenna Technol., Small Antennas Novel Metamater.*, Mar. 2005, pp. 69–72.
- [16] D. Hernandez, J. H. Seo, and K. N. Kim, "Linear array arrangement using composite right/left-handed transmission lines for magnetic resonance imaging," *Int. J. Imag. Syst. Technol.*, vol. 30, no. 1, pp. 216–223, 2020, doi: [10.1002/ima.22349](https://doi.org/10.1002/ima.22349).
- [17] J. T. Svejda, "An intrinsically double tuned half-wavelength CRLH resonator for combined  $^{23}\text{Na}/^1\text{H}$  MRI," *Magn. Reson. Phys. Biol. Med.*, vol. 26, no. 1, pp. 346–348, 2013.
- [18] J. Mosig, A. Bahr, T. Bolz, and A. Rennings, "Design and characteristics of a metamaterial transmit/receive coil element for 7 Tesla MRI," in *Proc. World Congr. Med. Phys. Biomed. Eng. (IFMBE)*, 2009, pp. 173–176, doi: [10.1007/978-3-642-03879-2\\_50](https://doi.org/10.1007/978-3-642-03879-2_50).
- [19] V. Panda, S. M. Sohn, J. T. Vaughan, and A. Gopinath, "A zeroth order resonant element for MRI transmission line RF coil," in *Proc. IEEE Int. Symp. Antennas Propag. (APSURSI)*, Jun./Jul. 2016, pp. 1389–1390.
- [20] A. Rennings, J. Mosig, A. Bahr, C. Caloz, M. E. Ladd, and D. Erni, "A CRLH metamaterial based RF coil element for magnetic resonance imaging at 7 Tesla," in *Proc. 3rd Eur. Conf. Antennas Propag.*, Mar. 2009, pp. 3231–3234.
- [21] C. Wang and G. X. Shen, "B1 field, SAR, and SNR comparisons for birdcage, TEM, and microstrip coils at 7T," *J. Magn. Reson. Imag.*, vol. 24, no. 2, pp. 439–443, Aug. 2006, doi: [10.1002/jmri.20635](https://doi.org/10.1002/jmri.20635).
- [22] M. Zubkov, A. A. Hurshkainen, E. A. Brui, S. B. Glybovski, M. V. Gulyaev, N. V. Anisimov, D. V. Volkov, Y. A. Pirogov, and I. V. Melchakova, "Small-animal, whole-body imaging with metamaterial-inspired RF coil," *NMR Biomed.*, vol. 31, no. 8, p. e3952, Aug. 2018, doi: [10.1002/nbm.3952](https://doi.org/10.1002/nbm.3952).
- [23] J. Gao and G. Lu, "CRLH transmission lines for telecommunications: Fast and effective modeling," *Int. J. Antennas Propag.*, vol. 2017, pp. 1–5, 2017, doi: [10.1155/2017/1592783](https://doi.org/10.1155/2017/1592783).
- [24] A. Christ, W. Kainz, E. G. Hahn, K. Honegger, M. Zefferer, E. Neufeld, W. Rascher, and R. Janka, "The virtual family—Development of surface-based anatomical models of two adults and two children for dosimetric simulations," *Phys. Med. Biol.*, vol. 55, no. 2, pp. N23–N38, 2010, doi: [10.1088/0031-9155/55/2/N01](https://doi.org/10.1088/0031-9155/55/2/N01).



**DANIEL HERNANDEZ** received the Ph.D. degree from Kyung Hee University, Republic of Korea, in 2016. He is currently working as a Research and Assistant Professor with the Department of Biomedical Engineering, Gachon University. His research interests include electromagnetic theory, simulations and development of antennas, and image and signal processing for MRI engineering.



**MINYEONG SEO** received the M.S. degree from the Department of Health Sciences and Technology, Gachon University, Incheon, Republic of Korea, in 2022. She is currently a Researcher with the Neuroscience Research Institute, Incheon. Her research interests include RF coil and electromagnetic simulation.



**YEJI HAN** received the Ph.D. degree in electrical engineering from the Korea Advanced Institute of Science and Technology, in 2007. She is currently an Associate Professor with the Department of Biomedical Engineering, Gachon University, Republic of Korea. Her research interests include medical imaging, magnetic resonance imaging, and image processing.



**KYOUNG-NAM KIM** received the Ph.D. degree in electrical engineering and information technology from the University of Duisburg-Essen, Germany, in 2011. He has been an Associate Professor with the Department of Biomedical Engineering, Gachon University, Incheon, Republic of Korea, since 2016. He is currently an MRI Committee Member of the Korean Society of Magnetic Resonance in Medicine. His research interests include medical electronic engineering, MRI systems, electromagnetic field analysis, and RF MRI coils.